Heliyon 7 (2021) e07083

Contents lists available at ScienceDirect

Heliyon

journal homepage: www.cell.com/heliyon

Research article

Cerebroprotective effect of pterostilbene against global cerebral ischemia in rats

Mohd Muazzam Khan [a], Badruddeen [a,*], Usama Ahmad [a], Juber Akhtar [a], Mohammad Irfan Khan [a], Mohd Faiyaz Khan [b]

[a] Faculty of Pharmacy, Integral University, Lucknow, 226020, Uttar Pradesh, India
[b] Department of Clinical Pharmacy, Prince Sattam Bin Abdul Aziz University, Al-Kharj, Saudi Arabia

ARTICLE INFO

Keywords:
Pterostilbene
Global cerebral ischemia
Neurobehavioral alterations

ABSTRACT

Aim of the study: The role of pterostilbene against induced neurobehavioral alterations in global cerebral ischemia-reperfusion and oxidative damage was studied.

Materials and methods: Male SD rats (180–200 g) were exposed for 30 min to bilateral carotid artery occlusion accompanied by 60 min reperfusion to cause cerebral injury. Pretreatment with pterostilbene (200 and 400 mg/kg, orally) was given to the animals for ten days followed by ischemia-reperfusion injury. Various behavioral tests (locomotor activity, neurological score, transfer latency, hanging wire test) were studied. The brain tissues of animals were used for both the biochemical parameters (lipid peroxidation, reduced glutathione, superoxide dismutase, catalase activity) and histopathological study.

Result: The pterostilbene as given orally significantly improved neurobehavioral alterations compared to control ischemia-reperfusion. Treatment with pterostilbene (200, and 400 mg/kg, orally) also significantly attenuated oxidative damage as indicated by reduced lipid peroxidation, nitrite concentration, restored reduced glutathione, and catalase activity as compared to control (ischemia-reperfusion) animals. Overall, pterostilbene treated animals showed non significant histological alteration as compared to ischemia-reperfusion control.

Conclusion: This work suggests the beneficial effect of pterostilbene and its therapeutic potential against reperfusion-induced ischemia and associated behavioral changes in rats due to the stabilization of DNA damage with significant free radical scavenging properties.

1. Introduction

Human brain shares only 2% of the total body weight. However, 25% of the whole body oxygen and glucose is utilized by brain to maintain electrical activity and functions [1]. Stroke is a global socio-economic issue that places a significant burden on patients, their families, and broader society [2]. Next to ischemic heart disease, it is the second leading cause of death. Further, it accounts for about 11% of mortality and the primary cause of morbidity. It is predicted that the top ten reason of death accounted for 55% of the 55.4 million global (WHO 2019). According to Global Burden of Diseases (2001) statistics, stroke incidence is increasing in low and middle-income countries (LMICs), which account for more than 85 % of all strokes, when compared with high-income countries (HICs) [3]. In India, stroke incidence is increasing significantly in recent times, with an increased life span [4].

According to the World Health Organization, over 15 million people a year, equating to one in every 400 people, suffer a stroke worldwide, out of which approximately 33.3% die, and among the survivor, 50% are left with permanent disabilities, placing a burden on family and community [5,6].

In cerebral ischemic conditions, blood flow to the brain is inadequate to meet the metabolic demand resulting in a reduced supply of oxygen or cerebral hypoxia and resulting in brain tissue death. Of all strokes, 87% are ischemic, 10% are intracerebral illnesses and 3% are subarachnoid hemorrhages. According to the WHO, stroke was the world's second most common cause of death and the third most common cause of death in developed countries [7,8,9,10,11].

Cerebral stroke pathophysiologic mechanisms include energy loss, free radical production, inflammation, intracellular Ca^{+2} level elevation, excitotoxicity and cell death via apoptosis or necrosis. In necrotic pathway cytoskeletal breakdown occurs rapidly due to energy failure or loss. While in the apoptotic pathway, the programmed death of cells occurs [12]. The depletion of glucose leads to the inability of mitochondria to produce ATP [13].

* Corresponding author.
E-mail address: badarmiracle@gmail.com (Badruddeen).

https://doi.org/10.1016/j.heliyon.2021.e07083
Received 9 February 2021; Received in revised form 26 March 2021; Accepted 12 May 2021
2405-8440/© 2021 Published by Elsevier Ltd. This is an open access article under the CC BY-NC-ND license (http://creativecommons.org/licenses/by-nc-nd/4.0/).

Due to the lack of ATP production, membrane function stops, and neurons become depolarized, and intracellular calcium level increases. Cell depolarization also causes the release of the excitatory neurotransmitter glutamate in the synaptic terminals causing excitotoxicity of the cells. Free radical species generated by mitochondrial dysfunction and membrane lipid degradation cause catalytic membrane degradation and damage other vital cellular functions. Oxygen free radicals serve as significant indicating molecules that generate inflammation and apoptosis [14] Stilbenes are phytochemicals with a molecular weight of ~200–300 g/mol, a subset of polyphenolic compounds [15].

Pterostilbene (3,5-dimethoxy-4-hydroxystilbene), a natural resveratrol dimethylated analog, found in berries, grapes, and grapevine, has been shown to possess antioxidant, anti-proliferative, anti-cancer, and anti-inflammatory activities in vitro and in vivo [16,17]. Pterostilbene is having low molecular weight, more lipophilic therefore it can be easily cross the blood-brain barrier, has greater bioavailability, and is more biologically active than resveratrol [18]. Therefore, in the present study, we first observe the preventive effect of pterostilbene and get a reference dose to observe further its therapeutic effect on acute focal cerebral I/R (Ischemic/Reperfusion) injury in a rat model. We thoroughly evaluate the therapeutic effect of pterostilbene on cerebral I/R injury, focusing on the recovery of neurological function, histological outcome, and BBB disruption. Furthermore, after cerebral I/R, we studied the effect of pterostilbene on oxidative stress and neuronal apoptosis in brain tissue.

2. Material and method

2.1. Drugs and chemicals

EDTA (ethylene diamine tetraacetic acid) and Sodium azide AR from SD fine chem ltd whereas DTNB (5,5-dithiobis (2-nitro benzoic acid)) and Thiobarbituric acid (TBA) from Himedia chemicals. Pterostilbene was obtained from Changsha Staherb Natural Ingredients Co., Ltd., China.

2.2. Pterostilbene and target protein structure retrieval

The three-dimensional structure of Pterostilbene [PubChem CID: 5281727] was obtained from the PubChem database. The target protein structure of Caspase 3, 8, and 9 were retrieved from Protein Data Bank [PDBID: 1GFW, 1QTN, 1NW9, respectively] for docking study.

2.3. Physicochemical properties and toxicity potential prediction

The physicochemical properties and toxicity potential of pterostilbene were estimated by Orisis Data warrior property explore tool (http://www.openmolecules.org/datawarrior/download.html).

Initially, different physicochemical parameters such as number of hydrogen bond acceptors and donors, cLogP value, molecular weight, number of rotatable bonds, topological polar surface area, and the Lipinski's rule violation [19] were calculated (Table 1). Subsequently % of Absorption was estimated by the method of Zhao et al., (2002) [20].

The Absorption % = 109 – (0.345 × TPSA). Prediction of toxicity was also evaluated by orisis data warrior tool, in which predictions are based on comparative analysis of our tested compounds with the pre-estimated set of known structural molecules. Mutagenicity, tumorogenicity, reproductive effects and irritability features of our tested compounds were predicted for toxicity assessment (Table 2).

Table 2. Toxicity potential of pterostilbene.

Compounds	Toxicity Risks			
	Mutagenic	Tumorigenic	Reproductive effect	Irritant
Pterostilbene	None	None	High	None

2.4. Molecular docking

Pterostilbene were considered as ligands and docked to target proteins Caspase 3, 8 and 9 as performed by Rizvi et al., (2013) [21]. Each ligand energy was minimized by MMFF94 force field, followed by adding gasteiger partial charges. Rotatable bonds were defined after adding non-polar hydrogen atoms. Hydrogen atoms, solvation parameters and Kollman united atom type charges were added by using AutoDock 4.2. Affinity (grid) maps of 60 × 60 × 60 Å grid points and 0.375 Å spacing were generated using the Autogrid program aimed to target grid co-ordinates in proximity with the catalytic site of Caspase3, Caspase8 and Caspase9, respectively. The values of x, y and z co-ordinates used for targeting the 'catalytic site of Caspase3' were 37.356, 35.146 and 27.054, respectively. While -8.572, 20.530, and 16.432 were the x, y and z co-ordinate used for targeting the 'catalytic site of Caspase8'. To target Caspase9, several docking experiments were performed by placing the center of the grid at different well-recognized amino acid residues. van der Waals and the electrostatic terms were calculated by applying default parameters and dielectric functions of AutoDock 4.2. 'Lamarckian genetic algorithm' and 'Solis and Wets local search method' was used to perform molecular docking experiments. Torsions, orientation and initial position for docking were fixed arbitrarily. One hundred different runs were applied for each docking experiment that was further set to end after 2, 500,000 energy evaluations. One hundred fifty were kept the population size. In the end, final AutoDock 4.2 figures were studied by using Discovery Studio 2.5 (Accelrys).

2.5. LIGPLOT^{+} analysis of docked results

After performing the docking, the best ligand-target confirmation was selected and analyzed by using LIGPLOT^{+} (Version v.2.1), LIGPLOT analysis. It is helpful to identify the hydrogen and hydrophobic interactions between important amino acid residues of the active site of Caspases and the tested compounds. The three-dimensional structures of ligand-target interaction generated were transformed into two-dimensional figures using the LIGPLOT algorithm.

2.6. Animals

Male SD rats (180–200 g) were procured from the National Laboratory Animal Centre, Central Drug Research Institute (CDRI), Lucknow.

Table 1. Physicochemical properties of Pterostilbene.

Compounds	Physiochemical parameters							
	% of Absorption*	Topological Polar Surface Area (Å)^2	Molecular Weight	cLogP**	Hydrogen Bond Donors	Hydrogen Bond Acceptors	Number of Rotatable Bonds	Lipinski's Violation
Rule	-	-	<500	≤5	<5	<10	≤10	≤1
Pterostilbene	95.65	38.69	256.30	3.38	1	3	4	0

* Percentage of Absorption (% of Absorption) was calculated by: % of Absorption = 109 – [0.345 × Topological Polar Surface Area].
** Logarithm of compound partition coefficient between *n*-octanol and water.

They were kept in the departmental animal house, Integral University, one week before the study (for acclimatization) and during the study under standard laboratory conditions, such as relative humidity (55–65%), temperature (23 ± 2 °C), and 12 h light/dark cycle, respectively and provided with standard rodent pellet diet and water *ad libitum*. An animal study was approved by the Institute Animal Ethics Committee, Integral University, Lucknow. Registration no. 1213/PO/RE/S/08/CPCSEA and approval no. IU/IAEC/18/36.

2.7. Experimental protocol

2.7.1. Drug treatment

Twenty-five male SD rats (180–200 g) were divided into five groups (n = 5, in each group). The animals in each group were fed with a drug or vehicle for ten days. The first group (i.e., sham controls) had anesthesia and access to surgery but it was not received an occlusion. The second group served as an ischemic control (i.e., diseased control group), that was subjected to ischemia-reperfusion, and were given 0.9% normal saline for ten days. Pterostilbene (200 and 400 mg/kg, suspended in 1% Tween 80) was administered orally for ten days before ischemic reperfusion (ischemia-reperfusion) induction in group 3 and group 4, respectively. The Quercetin (25 mg/kg, orally) was administered in group 5^{th} (served as a standard treated group).

2.7.2. Induction of cerebral ischemia/reperfusion (ischemia-reperfusion) injury in rats

Induction of cerebral ischemia/reperfusion was carried by a slight modified method [22]. Ketamine (45 mg/kg, i.p.) was used to anesthetize animals, and midline incision exposed both the common carotid arteries. The dissection was made between the sternocleidomastoid and the sternohyoid muscles parallel to the trachea.

Ischemia was induced by the occlusion of bilateral common carotid arteries (BCCAO) with clamps for 30 min followed by 60 min reperfusion. The skin was closed with stitches using silk suture Animals were observed during BCCAO for the following criteria: the absence of corneal reflex when exposed to intense light stimulation, maintenance of dilated pupils, and rectal temperature maintenance at (37 °C). 60 min after reperfusion period animals were evaluated for the neurological outcome and then sacrificed for biochemical and histological evaluation.

2.7.3. Measurement of locomotor activity (ambulation) by actophotometer

The locomotive activity (ambulatory activity) was recorded by Actophotometer (DECIBEL India). The animal was kept individually in the activity meter for 3 min for habituation. Then locomotive activity was recorded for 5 min. The ambulatory activity was noted and expressed in relation to total photo beam counts for each 5 min [23].

2.7.4. Elevated plus maze test for spatial memory

It consists of two opposite open arms (50 × 10 cm) which were connected by two closed arms of the same size with 40 cm walls. The arms were attached to the square of the middle (10 × 10 cm). Memory retrieval was tested on day 6, just before the surgery. The rat was individually placed at one end of an open arm facing off from the central square. In initial transfer latency (ITL), the time taken by the animal to move from the open arm and into one of the closed arms was reported. After recording ITL, Rat was allowed to explore the maze for 30 s and returned to the cage [23].

2.7.5. Hanging wire test

After ischemia-reperfusion mediated brain injury and to assess the rats griping and forelimb strength, hanging wire test was used [24] The ischemic animals (treated group and control group) were suspended from the forelimbs on a wire extended 60 cm above a foam pillow between 2 posts. The time (in s) has been recorded until the animal has fallen, and the cut-off time was 90 s.

2.7.6. Inclined beam walking test

An inclined beam walking test was used to determine motor coordination in the fore and hind limbs [25].

Each animal was positioned individually on a wooden bar, inclined from the platform at an angle of 60^0. Rats ' motor performance was scored on a scale from 0 to 4. The animal that could readily traverse the beam was given 0 scores. Animals displaying mild, moderate, and extreme disabilities were given scores 1, 2, and 3, respectively. The animals were assigned score 4, those totally unable to walk on the beam.

2.7.7. Biochemical estimations

2.7.7.1. Lipid peroxidation (LPO). 1 ml of brain homogenate was pipetted in a 20 ml glass vial and incubated for 60 min with 120 strokes up and down in a metabolic water bath shaker at 37 ± 1 °C. The other 1 ml was put in a centrifuge tube at 0 °C and labeled as 0 h of incubation. After 1 h incubation, in both samples, 1 ml of 0.67 percent TBA and 1 ml of 5 percent TCA were added, i.e. (0 h and 37 °C). The vial reaction mixture was transferred to the tube and centrifuged for 15 min at 3500 rpm. In another tube, the supernatant was transferred and kept for 10 min in a boiling water bath. The test tube was cooled now, and the absorbance was read at 535 nm. LPO rate was expressed as nM of the protein formed/h/mg TBARS reactive material [26].

2.7.7.2. Reduced glutathione (GSH). 1 ml PMS (10 percent, w/v) with 1 ml sulfosalicylic acid (4 percent) was precipitated. The samples were held for at least 1 h at 4 °C and then centrifuged for 15 min at 4 °C at 1200 rpm. The total volume of assay mixture contained a 3 ml of 0.1 ml of PMS (10 percent, w/v), 0.2 ml of DTNB (40 mg/10 ml of phosphate buffer, 0.1 M, pH 7.4), and 2.7 ml of phosphate buffer (0.1 M, pH 7.4). The established yellow color was immediately read at 412 nm. The activity of the enzymes was calculated as mm DTNB oxidized/min/mg of protein [27].

2.7.7.3. Catalase (CAT). The activity of catalase was spectrophotometrically assayed using the Aebi method [28]. The 3 ml assay mixture contained 0.063 percent H_2O_2 in 0.1 M KPB pH 7.4 and 10 ml supernatant tissue. The amelioration was recorded at 240 nm for 1 min. The function of the enzymes is expressed in mmol of H_2O_2 decomposed per minute per milligram of protein using a coefficient of molar extinction of 43.6 $M^{-1}cm^{-1}$. The activity was depicted as units of a protein per milligram.

2.7.7.4. Superoxide dismutase (SOD). The activity of superoxide dismutase in supernatant tissue was calculated by Marklund and Marklund process (Marklund and Marklund, 1974) [29]. The rate of auto-oxidation of pyrogallol inhibition was noted at 420 nm following the addition of enzyme extract. The amount of enzyme needed to give pyrogallol auto-oxidation inhibition of 50 percent was considered as one unit of enzyme activity. The function of the enzymes is expressed as unit protein per milligram.

2.7.7.5. Estimation of AchE. An isolated brain has been used for assessing activity with AChE. A known brain tissue weight was homogenized in a solution of 0.32 M sucrose to get a 10 percent homogenate. It was centrifuged at 3000 rpm for 15 min, followed by centrifugation at 10000 rpm for 10 min at a constant temperature of 4 °C. After centrifugation, 1 mL of supernatant was mixed with 9 mL of sucrose solution to get 1% of the post mitochondrial supernatant (PMS). In a cuvette, a reaction mixture containing 2.7 mL of phosphate buffer, 0.1 mL of DTNB, and 0.1 mL of 1 percent PMS was taken and pre-incubated for 5 min at 37 °C. By the addition of 0.1 mL acetylthiocholine iodide substrate reaction was initiated. The absorbance of the yellow-colored compound produced during the reaction was measured at 412 nm for a period of 3 min for every 1-minute interval [30,31]. Without 1 percent PMS, a blank was determined. AChE activity was determined using formula [R 1⁄4 (DA/min

assay volume)/(extinction coefficient mg of protein)], where; R 1⁄4 enzyme activity rate (nmol acetylthiocholine iodide hydrolyzed per mg of protein per min); extinction coefficient 1⁄4 13600/M/cm; and assay volume 1⁄4 3 mL.

2.8. Statistical analysis

The data were represented as mean ± S.E.M. for five rats. The analysis of variance (ANOVA) test was followed by individual comparison by Newman-Keuls test using Prism Pad software (Version 6.05) to determine the level of significance. The value of the probability ($P < 0.05$) was considered statically significant.

3. Results

3.1. Pterostilbene interaction with (Caspase3, 8 & 9) with the help of molecular docking technique

The present study was evaluated the interaction of Pterostilbene with Caspase3, Caspase8, and Caspase9 with the help of a molecular docking technique.

Pterostilbene was found to interact with 10 amino acids, namely, Met61, His121, Gly122, Phe128, Cys163, Thr166, Tyr204, Ser205, Trp206, and Arg207 of Capase3 (Table 3). Gly122 and Arg207 showed hydrogen bonding, while, Met61, His121, Phe128, Cys163, Thr166, Tyr204, Ser205, and Trp206 showed hydrophobic interactions with Pterostilbene (Figure 1). The free energy of binding (ΔG) and estimated inhibition constant (K_i) for the 'Pterostilbene –Caspase3-interaction' were determined to be -6.07 kcal/mol and 35.25 μM, respectively. The total intermolecular energy of docking for Pterostilbene –Caspase3-interaction was found to be -7.57 kcal/mol 'van der Waals', 'HydrogenBond' and 'Desolvation' energy components together contributed -7.14 kcal/mol while the 'Electrostatic' energy component was found to be -0.43 kcal/mol.

Pterostilbene was found to interact with 8 amino acids, namely, Asp438, Ile439, Leu440, Leu470, Arg471, Lys472, Lys473, and Leu474 of Caspase8 (Table 3). Asp438 and Leu440 were involved in hydrogen bonding, while Ile439, Leu470, Arg471, Lys472, Lys473, and Leu474 showed hydrophobic interactions with Pterostilbene (Figure 2). The free energy of binding (ΔG) and estimated inhibition constant (K_i) for the 'Pterostilbene –Caspase8-interaction' were determined to be -6.35 kcal/mol and 22.12 μM, respectively. The total intermolecular energy of docking for Pterostilbene and Caspase8 interaction was found to be -7.84 kcal/mol 'van der Waals', 'HydrogenBond' and 'Desolvation' energy components together contributed -7.62 kcal/mol while the 'Electrostatic' energy component was found to be -0.22 kcal/mol.

Pterostilbene was found to interact with 15 amino acids, namely, Asp186, Leu190, Arg193, Phe194, Leu197, Leu235, Phe283, Ile284, Gln285, Ser344, Tyr363, Val364, Leu367, Phe371, Phe413 of Capase9 (Table 3). Asp186, Leu190, Arg193, Phe194, Leu197, Leu235, Phe283, Ile284, Gln285, Ser344, Tyr363, Val364, Leu367, and Phe371 showed hydrophobic interactions with Pterostilbene (Figure 3). The free energy of binding (ΔG) and estimated inhibition constant (K_i) for the 'Pterostilbene and Caspase9 interaction' were determined to be -4.27 kcal/mol and 736.18 μM, respectively. The total intermolecular energy of docking for Pterostilbene and Caspase9 interaction was found to be -5.77 kcal/mol 'van der Waals,' 'HydrogenBond' and 'Desolvation' energy components together contributed -5.73 kcal/mol while the 'Electrostatic' energy component was found to be -0.04 kcal/mol.

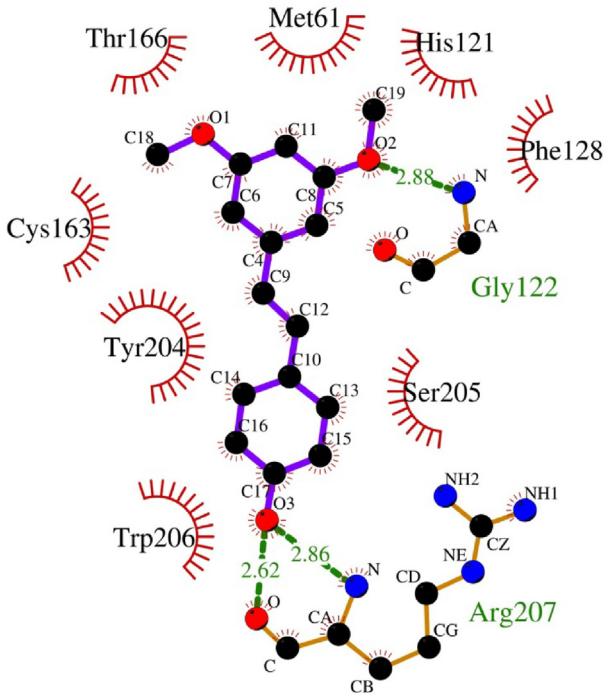

Figure 1. Ligplot analysis of Pterostilbene - Caspase 3 interaction. The amino acid residues forming hydrophobic interactions are shown as red arcs, while the hydrogen bonds are shown as green dashed lines with indicated bond lengths.

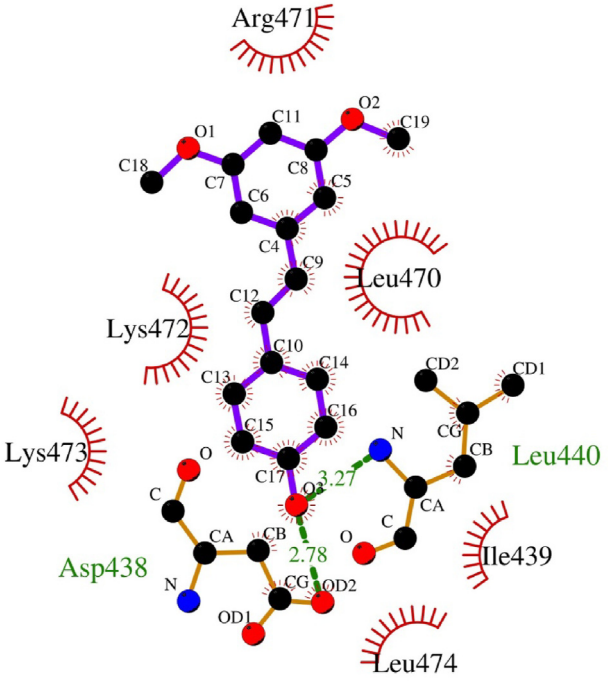

Figure 2. Ligplot analysis of Pterostilbene - Caspase 8 interaction. The amino acid residues forming hydrophobic interactions are shown as red arcs, while the hydrogen bonds are shown as green dashed lines with indicated bond lengths.

Table 3. Molecular docking results of Caspase 3, 8 and 9 interactions with Pterostilbene.

Compounds	Binding Energy (ΔG)	Inhibition Constant (Ki)	Interacting amino acids
Caspase 3	-6.07 kcal/mol	35.25 μM	Met61, His121, Gly122, Phe128, Cys163, Thr166, Tyr204, Ser205, Trp206, Arg207
Caspase 8	-6.35 kcal/mol	22.12 μM	Asp438, Ile439, Leu440, Leu470, Arg471, Lys472, Lys473, Leu474
Caspase 9	-4.27 kcal/mol	736.18 μM	Asp186, Leu190, Arg193, Phe194, Leu197, Leu235, Phe283, Ile284, Gln285, Ser344, Tyr363, Val364, Leu367, Phe371, Phe413

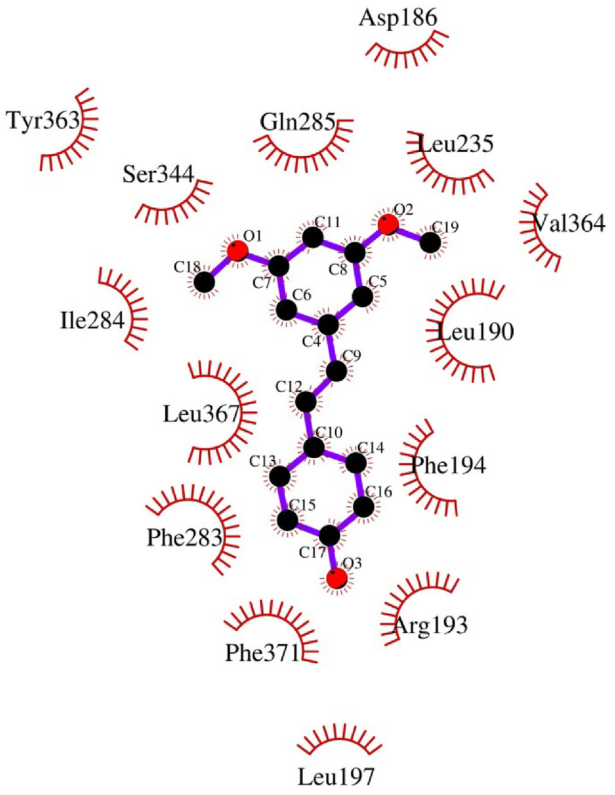

Figure 3. Ligplot analysis of Pterostilbene - Caspase 9 interaction. The amino acid residues forming hydrophobic interactions are shown as red arcs, while the hydrogen bonds are shown as green dashed lines with indicated bond lengths.

3.2. Effects of Pterostilbene on the neurological score of ischemia-reperfusion injured rats

Sham controlled animals displayed no impairment on motor control and neurological scores as compared with naive. Challenging the animals with 30 min of BCCAO followed by 60 min of reperfusion significantly elevated neurological score and induced motor coordination deficiency compared to the sham-controlled group. The animals treated with pterostilbene (200 mg/kg), (400 mg/kg) pretreatment was considerably improved neurological score and motor control as compared with the ischemic treated group and was equivalent to standard treated group Quercetin (25 mg/kg) (Figure 4).

3.3. Effects of Pterostilbene on locomotor activity of ischemia-reperfusion injured rats

Challenging the animals with 30 min of BCCAO followed by 60 min of reperfusion significantly impaired locomotor activity as compared to sham-treated rats ($P < 0.001$). Pretreatment with Pterostilbene (200 mg/kg and 400 mg/kg) substantially and dose-dependently ($P < 0.05$ to $P < 0.001$) increased locomotor activity relative to the ischemic control group (Figure 5).

3.4. Elevated plus maze test for spatial memory

Elevated plus maze test for spatial memory Initial transfer latency (ITL) did not differ significantly in any of the groups. Retention transfer latency (RTL) is significantly decreased in the sham group after 60 min of surgery, which indicates retention of memory. Challenging the animals with 30 min of BCCAO followed by 60 min of reperfusion produced a significant increase ($P < 0.001$) in the transfer latency time in elevated plus-maze as compared to sham-operated group I rats. Pretreatment with Pterostilbene (200 mg/kg and 400 mg/kg) showed a significantly

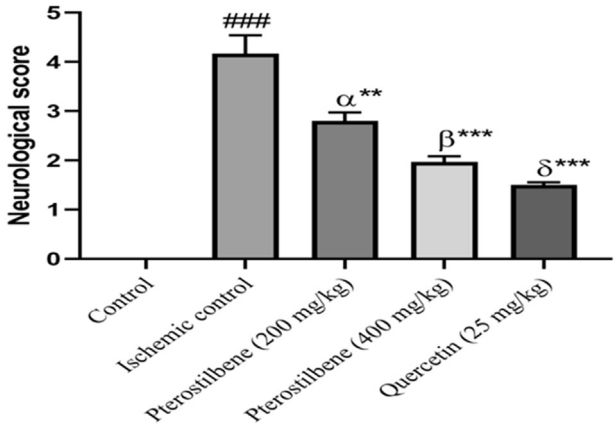

Figure 4. Effect of Pterostilbene on the neurological score. Data are shown as Mean ± S.E.M, $^{\#}P < 0.05$, $^{\#\#}P < 0.01$, $^{\#\#\#}P < 0.001$ and *<0.05, **<0.01, ***<0.001. $^{\#}$: Control vs Ischemic control; α: Ischemic control vs Pterostilbene (200 mg/kg); β: Ischemic control vs Pterostilbene (400 mg/kg); δ: Ischemic control vs Quercetin (25 mg/kg).

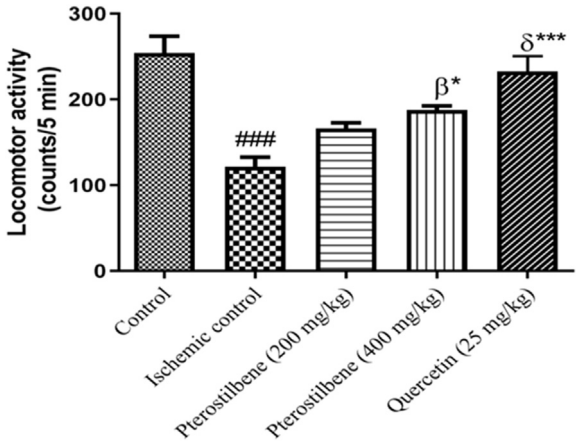

Figure 5. Effect of Pterostilbene on the locomotor activity. Data are shown as Mean ± S.E.M, $^{\#}P < 0.05$, $^{\#\#}P < 0.01$, $^{\#\#\#}P < 0.001$ and *<0.05, **<0.01, ***<0.001. $^{\#}$: Control vs Ischemic control; α: Ischemic control vs Pterostilbene (200 mg/kg); β: Ischemic control vs Pterostilbene (400 mg/kg); δ: Ischemic control vs Quercetin (25 mg/kg).

decrease ($P < 0.05$ to $P < 0.001$) in the transfer latency time as compared to the ischemia control group II. However, pterostilbene (400 mg/kg) significantly influence the transfer latency paradigm in the elevated plus-maze more than Quercetin (25 mg/kg) groups of rats (Figure 6).

3.5. Effect of pterostilbene on AchE activity

The AchE activity was increased in the ischemic group as compared to the control rats. It was decreased significantly in pterostilbene treated at a dose of 400 mg/kg as compared to the ischemic group and the result of Pterostilbene 400 mg/kg was similar as comparable to the Quercetin (25 mg/kg) treated group (Figure 7).

3.6. Effects of Pterostilbene on oxidative stress parameters of ischemia-reperfusion injured rats

Challenging the animals with 30 min of BCCAO followed by 60 min reperfusion significantly caused oxidative damage as indicated by increased ($P < 0.001$) LPO (lipid peroxidation), decreased ($P < 0.001$) CAT (catalase) and SOD (superoxide dismutase) ($P < 0.001$) activity of the brain as compared to sham-treated group I rats. Pre-treatment with pterostilbene (200 and 400 mg/kg) significantly restored depleted GSH (glutathione)

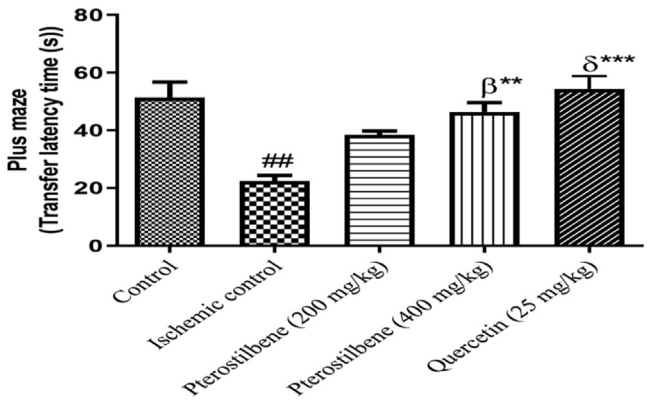

Figure 6. Effects of Pterostilbene on the Elevated plus maze test for spatial memory. Data are shown as Mean ± S.E.M, $^{\#}P < 0.05$, $^{\#\#}P < 0.01$, $^{\#\#\#}P < 0.001$ and *<0.05, **<0.01, ***<0.001. $^{\#}$: Control vs Ischemic control; α: Ischemic control vs Pterostilbene (200 mg/kg); β: Ischemic control vs Pterostilbene (400 mg/kg); δ: Ischemic control vs Quercetin (25 mg/kg).

and catalase activity as well as attenuated elevated lipid peroxidation (up to $P < 0.001$) of the brain, as compared to their respective control (ischemia/reperfusion group II rats) (Figures 8, 9, 10, 11).

4. Discussion

Cerebral ischemia leads to significant cognitive and behavioral disorders. In recent years, post-ischemia treatment and rehabilitation have gained that attention [32]. Pathophysiologically, ischemic stroke can be defined as brain tissue death due to temporary or permanent reduction in intracranial perfusion. It also decreased SOD, GSH, CAT level, and increased LPO as an index to measure the severity of oxidative damage in brain tissue produced by BCCAO [33].

Pterostilbene is a phytochemical stilbenoid with a resveratrol-like structure, pterostilbene (trans-3,5-dimethoxy-4′-hydroxystilbene) is composed of two extra methyl groups [34].

Pterostilbene is having low molecular weight, more lipophilic therefore it can be easily cross the blood-brain barrier, has greater bioavailability, and is more biologically active than resveratrol [35,36]. The brain is hugely susceptible to interruption of the blood supply without energy reserve. That may result in neuronal dysfunction and irreversible neural damage. The various types of glial cells (like astrocytes that coat 99% of the capillaries in the brain) extract glucose. This metabolised into

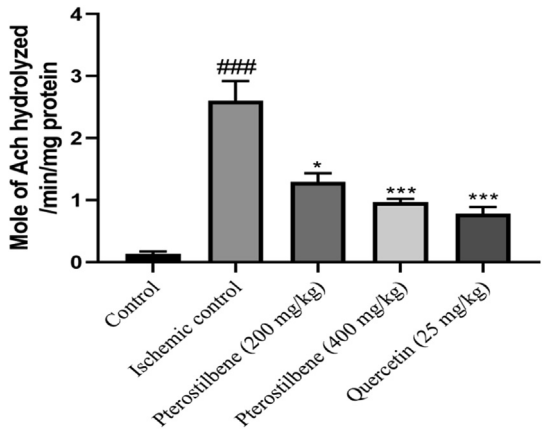

Figure 7. Effects of Pterostilbene on the AchE activity. Data are shown as Mean ± S.E.M, $^{\#}P < 0.05$, $^{\#\#}P < 0.01$, $^{\#\#\#}P < 0.001$ and *<0.05, **<0.01, ***<0.001. $^{\#}$: Control vs Ischemic control; α: Ischemic control vs Pterostilbene (200 mg/kg); β: Ischemic control vs Pterostilbene (400 mg/kg); δ: Ischemic control vs Quercetin (25 mg/kg).

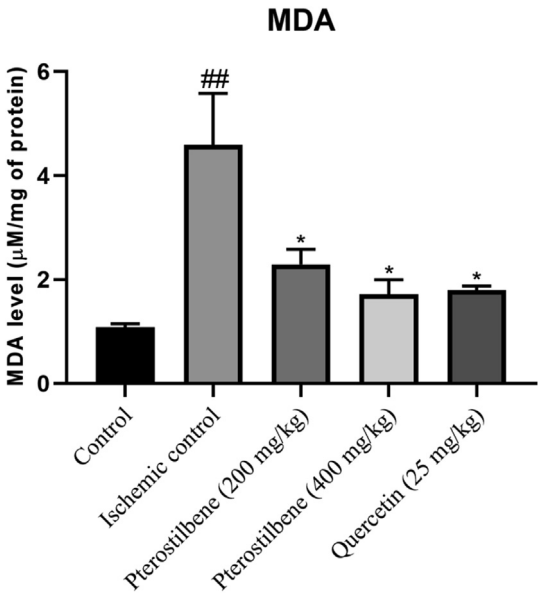

Figure 8. Effects of Pterostilbene on lipid peroxidation (LPO) (MDA μM/mg of protein). Data are shown as Mean ± S.E.M, $^{\#}P < 0.05$, $^{\#\#}P < 0.01$, $^{\#\#\#}P < 0.001$ and *<0.05, **<0.01, ***<0.001. $^{\#}$: Control vs Ischemic control; α: Ischemic control vs Pterostilbene (200 mg/kg); β: Ischemic control vs Pterostilbene (400 mg/kg); δ: Ischemic control vs Quercetin (25 mg/kg).

energy before it brought to neurons. Overall vascular endothelial cells and astrocytes are vital to neurons. Astrocytes unlike neurons are less vulnerable to glutamate toxicity during a brain stroke. However it induces astrogliosis. The reactive astrogliosis have been extensively related as a pathological attribute of transformed CNS tissues. That leads to glial scar creation and responsible for inhibition of axone regeneration, neurotoxicity, inflammation or chronic pain, augment pro inflammatory factors, reactive oxygen species (ROS), nitric oxide and glutamate [37]. In our work, pterostilbene inhibited ROS generation and acted as free

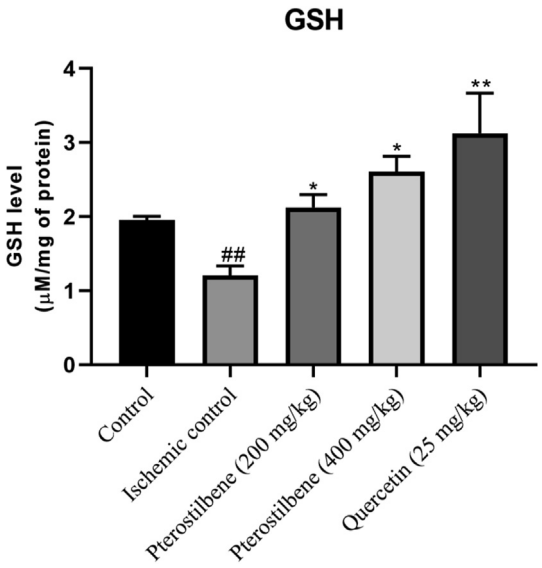

Figure 9. Effects of Pterostilbene on reduced glutathione (GSH) (μM/mg of protein),. Data are shown as Mean ± S.E.M, # Control vs Ischemic control. $^{\#}P < 0.05$, $^{\#\#}P < 0.01$, $^{\#\#\#}P < 0.001$ and *<0.05, **<0.01, ***<0.001. $^{\#}$: Control vs Ischemic control; α: Ischemic control vs Pterostilbene (200 mg/kg); β: Ischemic control vs Pterostilbene (400 mg/kg); δ: Ischemic control vs Quercetin (25 mg/kg).

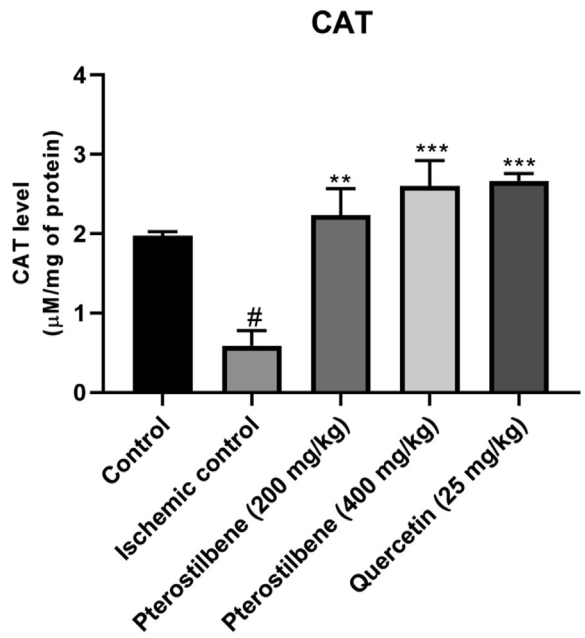

Figure 10. Effects of Pterostilbene on superoxide dismutase (SOD) (μM/mg of protein). Data are shown as Mean ± S.E.M, # Control vs Ischemic control. $^{\#}P < 0.05$, $^{\#\#}P < 0.01$, $^{\#\#\#}P < 0.001$ and *<0.05, **<0.01, ***<0.001. $^{\#}$: Control vs Ischemic control; α: Ischemic control vs Pterostilbene (200 mg/kg); β: Ischemic control vs Pterostilbene (400 mg/kg); δ: Ischemic control vs Quercetin (25 mg/kg).

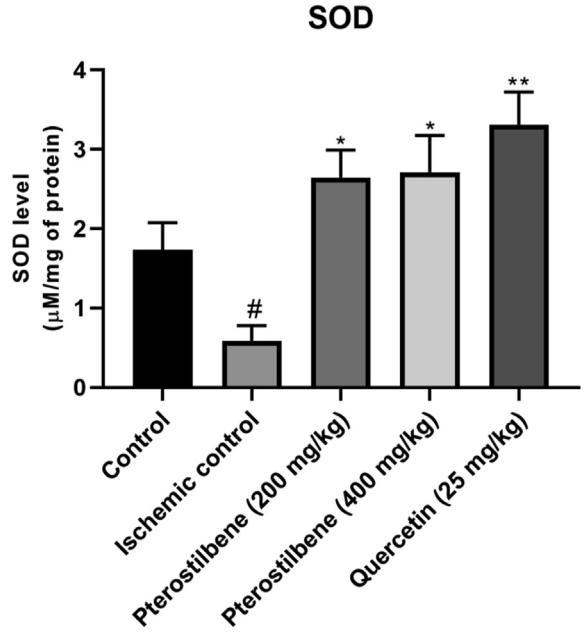

Figure 11. Effects of Pterostilbene on catalase (CAT) (μM/mg of protein). Data are shown as Mean ± S.E.M, $^{\#}P < 0.05$, $^{\#\#}P < 0.01$, $^{\#\#\#}P < 0.001$ and *<0.05, **<0.01, ***<0.001. $^{\#}$: Control vs Ischemic control; α: Ischemic control vs Pterostilbene (200 mg/kg); β: Ischemic control vs Pterostilbene (400 mg/kg); δ: Ischemic control vs Quercetin (25 mg/kg).

radical scavengers or antioxidants thereby protecting neurones and or astrocytes.

Pterostilbene has been shown to play a significant role as an antioxidant by up-regulating reversing cognitive behavioral deficits and releasing dopamine [38]. Besides, pterostilbene has been reported to possess anti-inflammatory activity [39], prevent dyslipidemia [40], anticancer [41] and anti-diabetic activity effects [42]. In this study, we observed pterostilbene's therapeutic potential on global cerebral ischemia-reperfusion injury in rats. Besides, our goal was to assess the brain damage caused by global cerebral ischemia and then observe the protective action of pretreatment with pterostilbene. The expression level of SOD, GSH, CAT and LPO was studied as an indicator of the severity of oxidative damage in brain tissue produced by BCCAO. All these parameters were markedly reversed and restored to near-normal levels in the groups pre-treated with pterostilbene.

Taken together, these data indicate that pterostilbene has antioxidant and free radical scavenging properties and the ability to modulate neurodegeneration induced oxidative damage in the brain, and can be used effectively as a neuroprotective adjuvant to eradicate oxidative stress. While pterostilbene has shown promising results in the global cerebral ischemia BCCAO model, further studies are needed to unravel the mechanism of action.

5. Conclusion

This study suggests the beneficial effect of pterostilbene and its therapeutic potential against reperfusion-induced ischemia and associated behavioral changes in rats due to the stabilization of DNA damage with significant oxidant inhibiting effects. As pterostilbene has antioxidant, free radical scavenging properties and modulates neurodegeneration-induced oxidative damage in the brain. Pterostilbene can be used effectively as a neuroprotective adjuvant to eradicate oxidative stress throughout in vivo ischemic injuries.

Declarations

Author contribution statement

Mohd Muazzam Khan:Performed the experiments; Wrote the paper.

Badruddeen: Conceived and designed the experiments; Analyzed and interpreted the data; Wrote the paper.

Usama Ahmad; Mohammad Irfan Khan: Contributed reagents, materials, analysis tools or data.

Juber Akhtar; Mohd Faiyaz Khan: Analyzed and interpreted the data.

Funding statement

This research did not receive any specific grant from funding agencies in the public, commercial, or not-for-profit sectors.

Data availability statement

Data included in article/supplementary material/referenced in article.

Declaration of interests statement

The authors declare no conflict of interest.

Additional information

No additional information is available for this paper.

Acknowledgements

Authors are highly thankful to the Prof. S.W. Akhtar, Hon'ble Chancellor Integral University and Prof. Syed Misbahul Hasan, Dean Faculty of Pharmacy, Integral University, Lucknow, India for providing with an academically rich environment and scientific facilities for the research in the university's infrastructure to explore and study extensively into clinically relevant fields. The Manuscript Communication Number

provided by the University for this Paper is IU/R&D/2021-MCN0001056. This publication is also supported by the deanship of scientific research at Prince Sattam bin Abdulaziz University, Alkharj, KSA.

References

[1] S. Nagahiro, M. Uno, K. Sato, S. Goto, M. Morioka, Y. Ushio, Pathophysiology and treatment of cerebral ischemia [In Process Citation], J. Med. Invest. (1998).

[2] J.K. Lovett, M.S. Dennis, P.A. Sandercock, J. Bamford, C.P. Warlow, P.M. Rothwell, Very early risk of stroke after a first transient ischemic attack, Stroke 34 (8) (2003) e138–e140.

[3] V.L. Feigin, C.M. Lawes, D.A. Bennett, S.L. Barker-Collo, V. Parag, Worldwide stroke incidence and early case fatality reported in 56 population-based studies: a systematic review, Lancet Neurol. 8 (4) (2009) 355–369.

[4] P.M. Dalal, S. Malik, M. Bhattacharjee, N.D. Trivedi, J. Vairale, P. Bhat, S. Deshmukh, K. Khandelwal, V.D. Mathur, Population-based stroke survey in Mumbai, India: incidence and 28-day case fatality, Neuroepidemiology (2008) 254–261.

[5] J.P. Broderick, Recanalization therapies for acute ischemic stroke, Semin. Neurol. (1998) 471–484.

[6] K. Mackay, J. Mensah, G A, S. Mendis, Greenlund, Types of cardiovascular disease, in: Atlas Hear. Dis. Stroke, 2004.

[7] E.H. Lo, T. Dalkara, M.A. Moskowitz, Mechanisms, challenges and opportunities in stroke, Nat. Rev. Neurosci. (2003) 399–414.

[8] U. Dirnagl, C. Iadecola, M. a Moskowitz, Pathobiology of ischaemic stroke, Trends Neurosci. (1999).

[9] M. R R, B.J. C, Pathophysiology of ischaemic stroke: insights from imaging, and implications for therapy and drug discovery, Br. J. Pharmacol. (2008) S44–S54.

[10] R.L. Martin, H.G.E. Lloyd, A.I. Cowan, The early events of oxygen and glucose deprivation: setting the scene for neuronal death? Trends Neurosci. (1994) 251–257.

[11] K.A. Hossmann, Viability thresholds and the penumbra of focal ischemia, Ann. Neurol. (1994) 557–565.

[12] U. Ziegler, P. Groscurth, Morphological features of cell death, Physiology 19 (2004) 124–128.

[13] H.W. Yung, A. Wyttenbach, A.M. Tolkovsky, Aggravation of necrotic death of glucose-deprived cells by the MEK1 inhibitors U0126 and PD184161 through depletion of ATP, Biochem. Pharmacol. 68 (2004) 351–360.

[14] B.A. Sutherland, J. Minnerup, J.S. Balami, F. Arba, A.M. Buchan, C. Kleinschnitz, Neuroprotection for ischaemic stroke: translation from the bench to the bedside, Int. J. Stroke (2012) 407–418.

[15] K. Roupe, C. Remsberg, J. Yanez, N. Davies, Pharmacometrics of Stilbenes: seguing towards the clinic, Curr. Clin. Pharmacol. (2008) 81–101.

[16] M.F. Lee, M.L. Liu, A.C. Cheng, M.L. Tsai, C.T. Ho, W.S. Liou, M.H. Pan, Pterostilbene inhibits dimethylnitrosamine-induced liver fibrosis in rats, Food Chem. (2013) 802–807.

[17] Y. Guo, L. Zhang, F. Li, C.P. Hu, Z. Zhang, Restoration of sirt1 function by pterostilbene attenuates hypoxia-reoxygenation injury in cardiomyocytes, Eur. J. Pharmacol. (2016) 25–33.

[18] I.M. Kapetanovic, M. Muzzio, Z. Huang, T.N. Thompson, D.L. McCormick, Pharmacokinetics, oral bioavailability, and metabolic profile of resveratrol and its dimethylether analog, pterostilbene, in rats, Canc. Chemother. Pharmacol. 68 (3) (2011) 593–601.

[19] C.A. Lipinski, Avoiding investment in doomed drugs Is poor solubility an industry wide problem? Curr. Drug Discov. (2001).

[20] Y.H. Zhao, M.H. Abraham, J. Le, A. Hersey, C.N. Luscombe, G. Beck, B. Sherborne, I. Cooper, Rate-limited steps of human oral absorption and QSAR studies, Pharm. Res. (N. Y.) 19 (10) (2002) 1446–1457.

[21] S.M.D. Rizvi, S. Shakil, M. Haneef, A simple click by click protocol to perform docking: autodock 4.2 made easy for non-bioinformaticians, Excli J. (2013) 831.

[22] Z.A. Shah, R.A. Gilani, P. Sharma, S.B. Vohora, Cerebroprotective effect of Korean ginseng tea against global and focal models of ischemia in rats, J. Ethnopharmacol. 101 (1-3) (2005) 299–307.

[23] D.S. Reddy, S.K. Kulkarni, Possible role of nitric oxide in the nootropic and antiamnesic effects of neurosteroids on aging- and dizocilpine-induced learning impairment, Brain Res. 799 (2) (1998) 215–229.

[24] A.J. Hunter, J. Hatcher, D. Virley, P. Nelson, E. Irving, S.J. Hadingham, A.A. Parsons, Functional assessments in mice and rats after focal stroke, Neuropharmacology 39 (5) (2000) 806–816.

[25] W.G. Dail, D.M. Fenney, H.M. Murray, R.T. Linn, M.G. Boyeson, Responses to cortical injury: II. Widespread depression of the activity of an enzyme in cortex remote from a focal injury, Brain Res. 211 (1) (1981) 79–89.

[26] E.D. Wills, Mechanisms of lipid peroxide formation in animal tissues, Biochem. J. 99 (3) (1966) 667–676.

[27] D. Jollow, J.R. Mitchell, N. Zampaglione, J.R. Gillette, Bromobenzene-induced liver necrosis. Protective role of glutathione and evidence for 3,4-bromobenzene oxide as the hepatotoxic metabolite, Pharmacology 11 (3) (1974) 151–169.

[28] H. Aebi, [13] catalase in vitro, Methods Enzymol. (1984) 121–126.

[29] S. Marklund, G. Marklund, Involvement of the superoxide anion radical in the autoxidation of pyrogallol and a convenient assay for superoxide dismutase, Eur. J. Biochem. 47 (3) (1974) 469–474.

[30] M. Shawwal, Badruddeen, M. Khushtar, M.A. Rahman, Protective effect of hydro-alcoholic extract of Salvia haematodes Wall root on cognitive functions in scopolamine-induced amnesia in rats, J. Tradit. Complement. Med. 7 (4) (2017) 471–475.

[31] G.L. Ellman, K.D. Courtney, V. Andres, R.M. Featherstone, A new and rapid colorimetric determination of acetylcholinesterase activity, Biochem. Pharmacol. 7 (2) (1961) 88–95.

[32] H.M. Bramlett, W.D. Dietrich, Pathophysiology of cerebral ischemia and brain trauma: similarities and differences, J. Cerebr. Blood Flow Metabol. 24 (2004) 133–150.

[33] K. Jeyaseelan, K.Y. Lim, A. Armugam, Neuroprotectants in stroke therapy, Expet Opin. Pharmacother. 9 (6) (2008) 887–900.

[34] A.M. Rimando, W. Kalt, J.B. Magee, J. Dewey, J.R. Ballington, Resveratrol, pterostilbene, and piceatannol in Vaccinium berries, J. Agric. Food Chem. 52 (15) (2004) 4713–4719.

[35] Y. Liu, Y. You, J. Lu, X. Chen, Z. Yang, Recent advances in synthesis, bioactivity, and pharmacokinetics of pterostilbene, an important analog of resveratrol, Molecules (2020) 5166.

[36] L. Deng, Y. Li, X. Zhang, B. Chen, Y. Deng, Y. Li, UPLC–MS method for quantification of pterostilbene and its application to comparative study of bioavailability and tissue distribution in normal and Lewis lung carcinoma bearing mice, J. Pharmaceut. Biomed. Anal. 114 (2015) 200–207.

[37] A. Becerra-Calixto, G.P. Cardona-Gómez, The Role of Astrocytes in Neuroprotection after Brain Stroke: Potential in Cell Therapy, 2017.

[38] J.A. Joseph, D.R. Fisher, V. Cheng, A.M. Rimando, B. Shukitt-Hale, Cellular and behavioral effects of stilbene resveratrol analogues: implications for reducing the deleterious effects of aging, J. Agric. Food Chem. 56 (22) (2008) 10544–10551.

[39] C.L. Hsu, Y.J. Lin, C.T. Ho, G.C. Yen, The inhibitory effect of pterostilbene on inflammatory responses during the interaction of 3T3-L1 adipocytes and RAW 264.7 macrophages, J. Agric. Food Chem. 61 (3) (2013) 602–610.

[40] A.M. Rimando, S.I. Khan, C.S. Mizuno, G. Ren, S.T. Mathews, H. Kim, W. Yokoyama, Evaluation of PPARα activation by known blueberry constituents, J. Sci. Food Agric. 96 (5) (2016) 1666–1671.

[41] A. Chakraborty, N. Bodipati, M.K. Demonacos, R. Peddinti, K. Ghosh, P. Roy, Long term induction by pterostilbene results in autophagy and cellular differentiation in MCF-7 cells via ROS dependent pathway, Mol. Cell. Endocrinol. 355 (1) (2012) 25–40.

[42] S. Gómez-Zorita, A. Fernández-Quintela, L. Aguirre, M.T. MacArulla, A.M. Rimando, M.P. Portillo, Pterostilbene improves glycaemic control in rats fed an obesogenic diet: involvement of skeletal muscle and liver, Food Funct 6 (6) (2015) 1968–1976.